The DEAD-box helicase Hlc regulates basal transcription and chromatin opening of stress-responsive genes

**Ruirui Jia[1],[†], Jiamei Lin[1],[†], Jin You[1],[†], Shi Li[1], Ge Shan[2] and Chuan Huang [1],***

[1]School of Life Sciences, Chongqing University, Chongqing 401331, China and [2]School of Basic Medical Sciences, Division of Life Science and Medicine, University of Science and Technology of China, Hefei 230027, China

ABSTRACT

Stress-responsive genes are lowly transcribed under normal conditions and robustly induced in response to stress. The significant difference between basal and induced transcription indicates that the general transcriptional machinery requires a mechanism to distinguish each transcription state. However, what factors specifically function in basal transcription remains poorly understood. Using a classic model stress-responsive gene (*Drosophila MtnA*), we found that knockdown of the DEAD-box helicase Hlc resulted in a significant transcription attenuation of *MtnA* under normal, but not stressed, conditions. Mechanistically, Hlc directly binds to the *MtnA* locus to maintain the accessibility of chromatin near the transcriptional start site, which allows the recruitment of RNA polymerase II and subsequent *MtnA* transcription. Using RNA-seq, we then identified plenty of additional stress-responsive genes whose basal transcription was reduced upon knockdown of Hlc. Taken together, these data suggest that Hlc-mediated basal transcription regulation is an essential and widespread mechanism for precise control of stress-responsive genes.

GRAPHICAL ABSTRACT
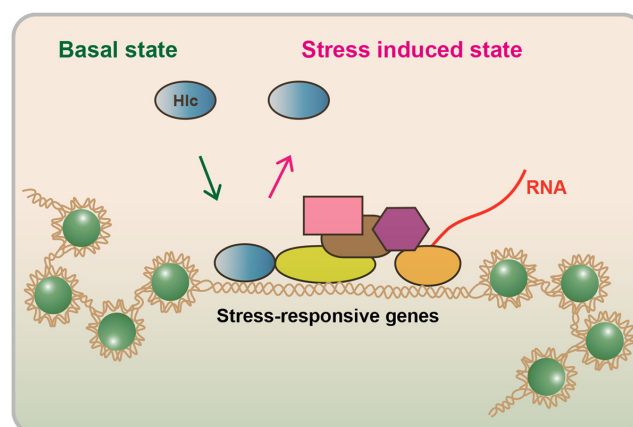
INTRODUCTION

External and internal stimuli provoke a significant transcriptional reprogramming, during which RNA polymerase II (Pol II) rapidly accumulates at the promoter and coding region of stress-responsive genes to enhance their expression (1,2). The adaptive transcription enables cells to respond within minutes upon exposure to various stresses, thereby improving cell survival and adaptation (1,2). For example, copper stress can quickly activate the transcription activity of *Drosophila* Metallothionein A (*MtnA*), whose encoded protein is able to sequester overloaded copper ions inside cells (3,4).

Note that a great many stress-responsive genes are not completely silent under normal conditions. Instead, they are continuously transcribed at the basal state, despite being at relatively low levels (1,2). Classic cases in point are *MtnA* and multiple heat shock protein genes (*Hsps*), whose basal expression can be readily detectable by different techniques (5–8). In particular, the basal activities of *Hsps* were found to have fundamental roles in normal cell growth and differentiation (9,10). These studies support that the basal

---

transcription program of stress-responsive genes is also an essential aspect of biological processes in living cells.

To date, most transcription factors identified function in both basal and stress-induced transcription. For example, the metal-responsive transcription factor-1 (MTF-1) is indispensable for the transcription activity of *MtnA* under both normal and heavy metal stressed conditions (11–14). Given the significant difference between basal and stress-induced transcription, we speculate that cells may require sophisticated mechanisms to assist the general transcriptional machinery and/or transcription factors to distinguish between normal and stressed conditions. In support, our previous study has demonstrated that knockdown of *Drosophila* gawky significantly reduced the level of metal-induced transcription but had no effect on basal transcription (15). Mechanistically, gawky translocates into the nucleus and directs the metal-activated version of MTF-1 to the promoter regions of metal-responsive genes to promote their transcription in response to heavy metal stress (15). This suggests that gawky is specific for dictating metal-induced transcription. However, what factors exclusively regulate basal transcription and the detailed mechanism remain an outstanding question.

Drosophila Hlc and its mammalian homolog DDX56 belong to DEAD-box helicases, a highly-conserved RNA-binding protein family whose members are involved throughout cellular RNA metabolism, such as splicing, nuclear export, translation and degradation (16–18). DDX56 was first identified as a ribosome biogenesis factor modulating the assembly process of the late-stage 60S ribosomal subunit in human and yeast cell lines (19,20). Consistently, loss of planarian DDX56 induces ribosome biogenesis disruption and leads to dysregulation of ribosomal proteins, which ultimately impairs cell proliferation and triggers caspase-dependent apoptosis (21). DDX56 was also found to exert an inhibitory or promoting effect on infectivity of various viruses (22–25). In the case of the West Nile virus (WNV), DDX56 directly binds to the capsid protein to form a stable complex which facilitates packaging of the infectious WNV into particles (22). By contrast, DDX56 attenuates infection of the chikungunya virus (CHIKV) by destabilizing incoming CHIKV genomic RNAs as well as reducing CHIKV protein production on early steps of viral replication (23). Moreover, recent studies have revealed the oncogenic roles of DDX56 in different cancer types (26–28). For example, DDX56 can promote tumor growth by affecting the alternative splicing of a subset of cell cycle-related genes in colorectal cancer (26). Although emerging roles of DDX56 have been revealed, studies regarding the molecular functions of this helicase are still very limited.

Using a classic model stress-responsive gene (*MtnA*), we here identified *Drosophila* Hlc as an essential regulator specific for dictating basal transcription. Mechanistically, Hlc directly interacts with the genomic locus of *MtnA* to maintain its open chromatin status. Knockdown of Hlc resulted in a condensed chromatin architecture near the transcriptional start site (TSS), thereby disassociating Pol II from the genomic *MtnA*. In addition, we found a negative cooperativity between gawky and Hlc at the genomic locus of *MtnA* during the transition from the basal to copper-induced transcription, confirming the specificity of Hlc-

meditated regulation. Using RNA-seq, we found plenty of additional stress-responsive genes whose basal transcription was significantly down-regulated upon knockdown of Hlc. Focused studies on heat stress genes further verified the general role of Hlc in basal transcription. In summary, we proposed that Hlc-mediated regulation acts as an essential and widespread mechanism to coordinate the basal transcription of stress-responsive genes.

MATERIALS AND METHODS

Drosophila cell culture and RNAi

Drosophila Schneider 2 (S2) cells were maintained in Schneider's *Drosophila* Medium (Sigma, S9895) containing 10% fetal bovine serum (v/v; Excell, FSP500) and 1% penicillin-streptomycin (v/v; Thermo Fisher Scientific, 15140122) at 25°C. DNA templates for double-strand RNA (dsRNA) preparation were obtained by PCR reactions with primer pairs containing the T7 promoter sequence (Supplementary Table S1). DsRNAs were generated by *in vitro* transcription using ScriptMAX® Thermo T7 Transcription Kit (TOYOBO, TSK-101). For Hlc RNAi in S2 cells, 1.5×10^6 cells were incubated with 8 μg of the indicated Hlc dsRNA in 600 μl of serum-free medium for 30 min at room temperature. After addition of 400 μl of medium containing 20% fetal bovine serum (v/v), dsRNA-treated cells were cultured at 25°C for 3 days. β-gal dsRNA served as a negative RNAi control in this study. To activate metal-induced transcription, where indicated, a final concentration of 500 μM copper sulfate (CuSO₄, Macklin, C805782) was added into the medium for the final 12 hr before collection. To activate heat shock-induced transcription, where indicated, cells were cultured at 33 or 37°C for the final 1 hr before collection.

Vector transfection, rescue assay and stable cell line construction

To generate Hlc expression vectors for transfection into *Drosophila* S2 cells, the indicated sequences were inserted into our previously described Hy_pAct5C FLAG MCS vector (15,29,30), a reporter which can express a FLAG-tagged protein under control of the *Act5C* promoter. These Hlc expression vectors were used for stable cell line construction and rescue assays. The detailed information of all vectors used in this study is provided in Supplementary Vector Information.

For transient transfection, 1μg of the indicated vector was introduced into 1.0×10^6 S2 cells using Lipo6000™ Transfection Reagent (Beyotime, C0526), and transfected cells were cultured at 25°C for 2 days before collection. For Hlc rescue assay, 24 hr after treatment with the Hlc UTR dsRNA, cells were transfected with the indicated Hlc vector and cultured at 25°C for another 4.5 days in the presence of 150 μg/ml hygromycin B (Biofroxx, 1366ML010). Note that these Hlc expression vectors only harbor the coding region and are insensitive to UTR dsRNA-mediated Hlc knockdown. For stable cell line construction, transfected cells were selected in the medium containing 150 μg/ml hygromycin B for 4 weeks.

RT-qPCR

RNA was isolated using RNAiso Plus (Takara, 9109), and complementary DNA (cDNA) was produced through reverse transcription (RT) using PrimeScript RT Master Mix Kit (Takara, RR036A) according to the manufacturer's instructions. Quantitative PCR (qPCR) was carried out with the indicated primer pairs and Hieff® qPCR SYBR Green Master Mix (YEASEN, 11201ES03) using the CFX connect real-time PCR system (Bio-Rad). Ct values were normalized to *rp49* mRNA expression. The sequences of all qPCR primers are provided in Supplementary Table S2.

Fluorescence *in situ* hybridization (FISH)

Fluorescent RNA probes were generated by *in vitro* transcription (ScriptMAX® Thermo T7 Transcription Kit, TOYOBO, TSK-101) and labeled with the Alexa Fluor 488 dye (ULYSIS Nucleic Acid Labeling Kit, Thermo Fisher Scientific, U21650). The sequence of the MtnA fluorescent probe is provided in Supplementary Table S3. FISH was conducted as previously described with minor modifications (15). In brief, cells were fixed by fixative solution (75% methanol (v/v) and 25% glacial acetic acid (v/v)) at room temperature for 10 min, denatured at 80°C for 10 min, incubated with 100 ng of denatured probes in the presence of 20 ng/μl yeast RNA (Beyotime, R0038) at 42°C overnight and stained with 1 μg/ml DAPI (Beyotime, C1002) for 5 min before confocal microscopy analyses. Fluorescence signals were detected using the Leica TCS SP8 system and quantified using ImageJ.

Nuclear run-on (NRO)

NRO assay was used to measure the production of the nascent *MtnA* transcript in *Drosophila* nuclei. NRO was performed as previously described (15,30). In brief, a total of 1.5×10^8 S2 cells were washed twice with 1 ml of ice-cold $1\times$ PBS buffer (phosphate buffer saline pH 7.4: 137 mM NaCl, 2.7 mM KCl, 10 mM Na_2HPO_4 and 1.8 mM KH_2PO_4) and resuspended into 5 mL of ice-cold Hypotonic Buffer (150 mM KCl, 4 mM MgOAc and 10 mM Tris–HCl pH 7.4) containing 80 units/ml RNase inhibitor (Beyotime, R0102). After 10 min incubation on ice, cells were collected by centrifugation at 1000g and resuspended into 1 ml of ice-cold Lysis Buffer (Hypotonic Buffer supplemented with 0.5% NP40 (v/v) and 80 units/ml RNase inhibitor) followed by ∼20 rounds of slow pipetting. Nuclei were then isolated by density gradient centrifugation using 4.5 ml of 0.6 M sucrose, resuspended into 100 μl of NRO Buffer (50 mM Tris–HCl pH 7.5, 5 mM $MgCl_2$, 150 mM KCl, 0.1% srkosyl (w/v), 10 mM dithiothreitol and 80 units/ml RNase Inhibitor) containing each of 1 mM NTPs (ATP, GTP, CTP and BrUTP (Sigma, B7166)) and incubated at 28°C for 5 min to allow incorporation of BrUTP into nascent transcripts. The NRO reaction was shut off by addition of 500 μl of RNAiso Plus (Takara, 9109). After RNA isolation, nuclear RNA was resuspended into 500 μl of RNA Immunoprecipitation Buffer (20 mM Tris–HCl, pH 7.5, 200 mM NaCl, 2.5 mM $MgCl_2$, 0.5% NP40 (v/v) and 10% glycerol (v/v)). BrUTP-labeled transcripts were then purified using Dynabeads® Protein G (Thermo Fisher

Scientific, 10003D) and anti-BrUTP (Abcam, ab1893). Efficient nascent RNA purification was verified by measuring the level of the *MtnA* precursor mRNA by RT-qPCR analysis.

Chromatin immunoprecipitation (ChIP)

ChIP was used to evaluate Pol II, Hlc and gawky density at the genomic locus of *MtnA*. A total of 7.5×10^7 S2 cells were washed twice with $1\times$ PBS (phosphate buffer saline pH 7.4: 137 mM NaCl, 2.7 mM KCl, 10 mM Na_2HPO_4 and 1.8 mM KH_2PO_4) containing 1 mM phenylmethanesulfonyl fluoride (PMSF) and cross-linked with 1% formaldehyde for 10 min at 37°C. The cross-linking reaction was stopped by addition of a final concentration of 125 mM glycine. Fixed cells were collected by centrifugation at 300g for 5 min, resuspended into ChIP Lysis Buffer (1% sodium dodecyl sulfate (SDS; w/v), 10 mM EDTA, 50 mM Tris–HCl pH 8.1 and 1 mM PMSF) and sonicated using a Scientz-IID Sonicator to yield 200–500 bp DNA fragments. The mixture was then centrifuged at 12 000g for 10 min at 4°C to remove cell debris, and the supernatant was saved as chromatin solution. 5% of the chromatin solution was used as the input sample, and the remaining was immunoprecipitated with the indicated antibody using ChIP Assay Kit (Beyotime, P2078) according to the manufacturer's instructions. These antibodies were used in ChIP: anti-FLAG (Beyotime, AF519), anti-Hlc (purified from rabbit antisera, raised against amino acids 545–560 of the endogenous *Drosophila* Hlc), anti-gawky (previously described in (15)) and anti-RNA polymerase II (Abcam, ab5095; this antibody recognizes Pol II phosphorylated at the serine 2 residue of the C-terminal domain repeat YSPTSPS). Note that a negative IgG (Beyotime, A7028) was also used in each ChIP experiment to exclude the potential of non-specific binding. DNA from the input and ChIP samples was purified using Cycle Pure Kit (OMEGA, D6492) and subjected to qPCR analysis. For Hlc and gawky ChIP, the DNA binding sites of Hlc and gawky (as well as the negative IgG) were defines as genomic regions enriched over the input DNA. For Pol II ChIP, signals (relative to input) were normalized to signals obtained from the negative IgG, and the normalized ChIP signal in the RNAi control sample was set to '1'.

Micrococcal nuclease (MNase) protection assay

MNase protection assay was used to examine the role of Hlc in chromatin accessibility. After RNAi and/or rescue experiments, a total of 1.5×10^8 S2 cells were washed twice with $1\times$ PBS buffer (phosphate buffer saline pH 7.4: 137 mM NaCl, 2.7 mM KCl, 10 mM Na_2HPO_4 and 1.8 mM KH_2PO_4), cross-linked with 1% formaldehyde in $1\times$ PBS buffer for 10 min and quenched with 125 mM glycine for 10 min. Fixed cells were then resuspended into 2 ml of ice-cold solution I (10 mM HEPES pH 7.6, 10 mM KCl, 1.5 mM $MgCl_2$, 0.34 M sucrose, 10% glycerol (v/v), 1 mM dithiothreitol, 0.1% Triton X-100 (v/v) and $1\times$ protease inhibitor cocktail (Beyotime, P1045)) followed by ∼50 rounds of slow pipetting. Nuclei were collected by centrifugation at 1000g for 5 min and resuspended into 1 ml of Solution II (3 mM EDTA, 0.2 mM EGTA, 1 mM dithiothreitol and $1\times$ protease inhibitor cocktail). After 30 min incubation on ice,

released chromatin was washed twice with 1mL of Solution II, resuspended into 1 mL of MNase Buffer (50 mM Tris–HCl pH 7.4, 25 mM KCl, 12.5% glycerol (v/v), 10 mM $CaCl_2$, 4 mM $MgCl_2$ and 1 mM PMSF) and then divided into two equal aliquots (0.5 ml). One was incubated with 5 units MNase (Aladdin, 9013-53-0) for 5 min at $37°C$, and the other, as the negative control sample (undigested), was lightly sonicated at 27% amplitude for 6 rounds of 24 s using a Scientz-IID Sonicator. Both aliquots were incubated at $65°C$ for 6 h and treated with 0.5 mg/ml proteinase K (Beyotime, ST535) for 30 min at $55°C$ to release the cross-linked DNA. After DNA purification, qPCR experiments were performed to quantify the extent of MNase digestion with 7 overlapping amplicons tiling through the genomic region of *MtnA* (–250 to +257 bp relative to the TSS). The relative protection level at each examined site was defined as the ratio of MNase-digested to undigested genomic DNA.

Immunofluorescence staining (IF)

IF was used to visualize the nuclear-cytoplasmic distribution of the wild-type and mutant Hlc. IF was performed as previously described (15,30,31). In brief, after treatment with fixative solution (75% methanol (v/v) and 25% glacial acetic acid (v/v)), fixed cells were permeabilized with 0.1% Triton X-100 (v/v) in TBST buffer (Tris-Buffered Saline Tween-20 pH 7.6: 0.242% Tris–HCl (w/v), 0.8% NaCl (w/v) and 0.05% Tween-20 (v/v)) at room temperature for 10 min and incubated with the indicated primary antibody in the presence of 5% bovine serum albumin (w/v; Beyotime, ST025) at $4°C$ overnight. After incubation with the fluorophore-conjugated secondary antibody, 1 µg/ml DAPI (Beyotime, C1002) was used to stain nuclei for 5 min before confocal microscopy analyses. Fluorescence signals were detected using the Leica TCS SP8 system and quantified using Image J. Line profiles were analyzed using Image-Pro Plus 6.0. These antibodies were used in IF: anti-Hlc (raised against amino acids 545–560 of the endogenous *Drosophila* Hlc), anti-FLAG (Beyotime, AF519), Alexa Fluor 555-labeled anti-mouse IgG (Beyotime, A0460) and Alexa Fluor 555-labeled anti-rabbit IgG (Beyotime, A0453).

Western blotting

Protein extracts from β-gal (the RNAi control) and Hlc RNAi cells were prepared using RIPA buffer (50 mM/l Tris–HCl pH 7.4, 150 mM/l NaCl, 0.1% SDS (w/v), 1% sodium deoxycholate (w/v) and 1% Triton X-100 (v/v)). Western blotting experiments were performed according to the standard ECL protocol (Thermo Fisher Scientific, EI9051). Antibodies used were anti-Hlc (raised against amino acids 545–560 of the endogenous *Drosophila* Hlc), anti-α-Tubulin (Beyotime, AT819), HRP-labeled goat anti-rabbit IgG (H + L) (Beyotime, A0208) and HRP-labeled goat anti-mouse IgG (H + L) (Beyotime, A0216).

RNA sequencing (RNA-seq) and bioinformatic analysis

Whole-cell RNA was isolated from two biological replicates using RNAiso Plus (Takara, 9109), and RNA quality was verified using the Agilent Bioanalyzer 2100 system.

RNA-seq libraries were generated with 1 µg of RNA using the Illumina TruSeq™ RNA Sample Preparation kit and were subject to 150 bp paired-end sequencing using the Illumina NovaSeq 6000 system. Adapter sequences and low-quality reads were removed with Trimmomatic (version 0.36) with parameters LEADING:3 TRAILING:3 SLIDINGWINDOW:4:15 MINLEN:36 (32). The remaining high-quality reads were then aligned to the reference genome (the *Drosophila melanogaster* genome (BDGP6)) from Ensembl (https://www.ensembl.org) using TopHat (version 2.1.0) (33,34). StringTie (version 2.1.7) was used to estimate global gene expression of each sample based on the Ensembl gene annotation (BDGP6.32, version 104) (33,35). Differential gene expression (DGE) analysis was performed using the DEseq2 R package (version 1.32) (36), and gene ontology (GO) analysis was performed using DAVID bioinformatics resources (2021 update) (37).

For ATAC-seq data analysis, the raw data, generated from *Drosophila* S2 cells, were downloaded from the Gene Expression Omnibus (GEO) repository (GSE197224, SRX10915169) (38), quality-trimmed using Trimmomatic (version 0.36) (32) and mapped to the *Drosophila melanogaster* genome (BDGP6) using TopHat (version 2.1.0) (33,34). Sambamba (version 0.8.1) was used to remove duplicate reads from the BAM file (39). The bigWig file with RPKM normalization was generated from the trimmed BAM file using deepTools (version 3.3.0) with the option 'computeMatrix' (40). The density plot reflecting ATAC-seq signals was generated using deepTools (version 3.3.0) with the option 'computeMatrix reference-point' (40).

Statistical analysis

Unless otherwise indicated, statistical significances were evaluated by Student's *t*-test. Statistical details are provided in each figure legend.

RESULTS

Identification of the role of Hlc in the mRNA expression of *MtnA*

To identify factors that specifically regulate the basal transcription of stress-responsive genes, we utilized the previously published screening dataset (15). Among all 127 factors screened, the DEAD-box helicase Hlc was the only candidate that modulated the expression level of *MtnA* (a well-characterized metal-responsive gene that belongs to the metallothionein family (41)) under normal, but not copper-stressed, conditions in *Drosophila* S2 cells (15). To ascertain the phenotype from the screening and exclude the possibility of off-target effects of RNAi-mediated transcript knockdown, we took advantage of 3 independent dsRNAs to individually reduce Hlc expression in unstressed and copper-treated S2 cells (Figure 1A, B; Supplementary Figure S1A). Consistently, the level of *MtnA* mRNA was significantly down-regulated under normal conditions, but had almost no change in response to copper treatment (Figure 1B). RNA-FISH of *MtnA* mRNA further verified the function of Hlc in *MtnA* expression at the single-cell level (Figure 1C, D).
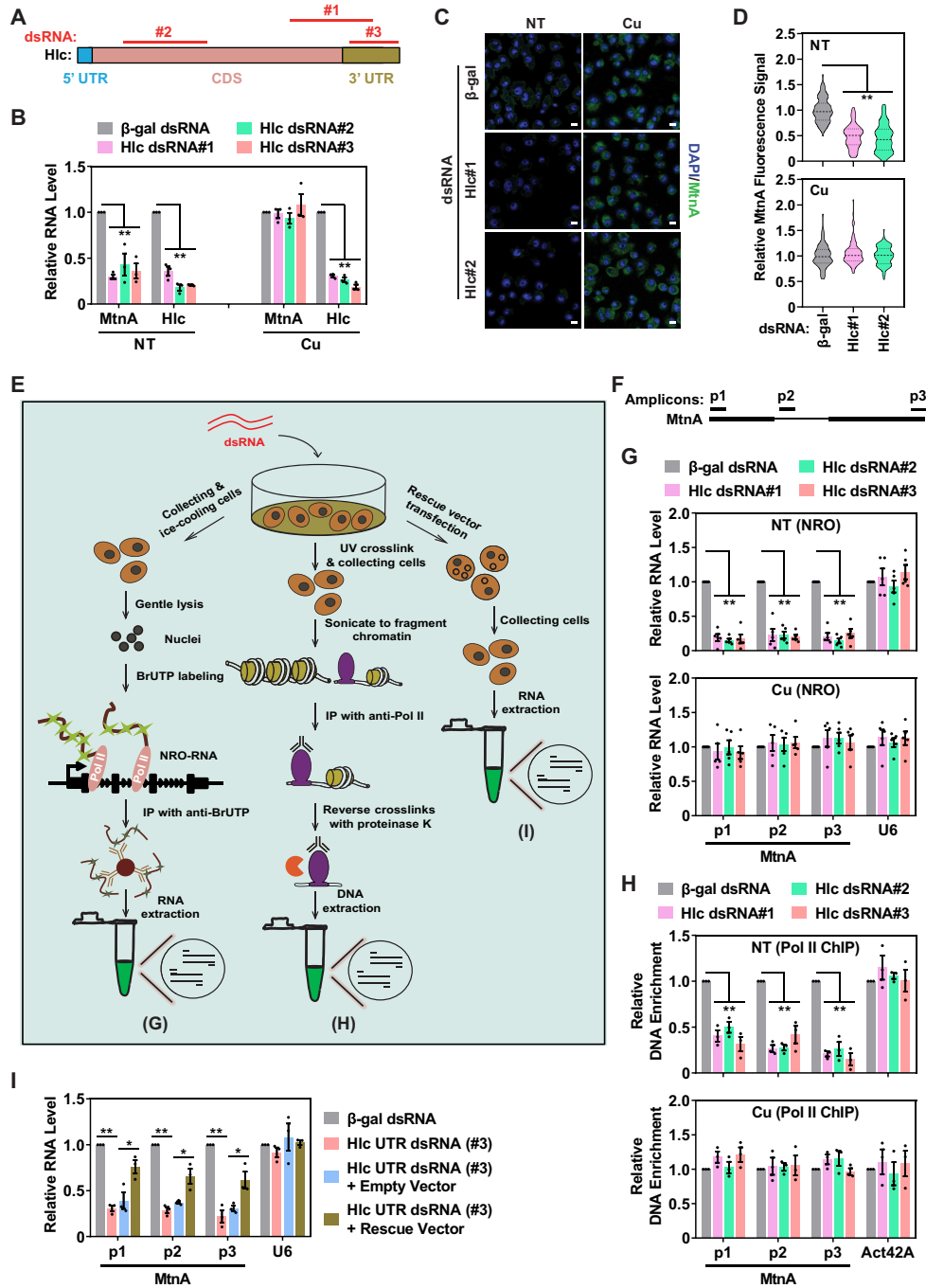
Figure 1. Hlc-mediated regulation is required for basal transcription but is bypassed for stress-induced transcription. (**A**) A schematic representation of the endogenous *Drosophila Hlc* mRNA and the approximate targeted positions of three independent Hlc dsRNAs. (**B**) RT-qPCR quantification of *MtnA* and *Hlc* expression using whole-cell RNA extracts purified from the control (β-gal) or Hlc RNAi cells (*n* = 3 biological replicates; each replicate present as a black dot). ∗∗*P* < 0.01; ∗*P* < 0.05, calculated by Student's *t*-test. (**C**) Confocal microscopy analysis of the *MtnA* FISH signals after Hlc RNAi. Representative images from 4 biological replicates are shown. Scale bar = 5 μm. (**D**) Violin plots comparing the *MtnA* FISH signals from samples described in Figure 1C (*n* = 100 cells for fluorescence signal quantification per sample). Lines inside each violin plot represent the first quartile, median and third quartile of the data. ∗∗*P* < 0.01; ∗*P* < 0.05, calculated by Student's *t*-test. (**E**) A schematic overview of the experimental setup (NRO, Pol II ChIP and rescue assay) for the data shown in (G)–(I). (**F**) The approximate locations of primer pairs detecting the 5′ end, middle or 3′ end of the *MtnA* gene body. (**G**) NRO analysis of the nascent *MtnA* transcript abundance (i.e. the transcription activity of *MtnA*) after Hlc RNAi (*n* = 5 biological replicates; each replicate present as a black dot). The reference gene *U6* served as a negative control. ∗∗*P* < 0.01; ∗*P* < 0.05, calculated by Student's *t*-test. (**H**) Pol II ChIP assay measuring Pol II density at the locus of *MtnA* after Hlc RNAi (*n* = 3 biological replicates; each replicate present as a black dot). The reference gene *Act42A* served as a negative control. ∗∗*P* < 0.01; ∗*P* < 0.05, calculated by Student's *t*-test. (**I**) RT-qPCR quantification of *MtnA* expression using whole-cell RNA extracts purified from the control RNAi, Hlc RNAi, empty vector control rescued or Hlc vector rescued cells (*n* = 3 biological replicates; each replicate present as a black dot). The reference gene *U6* served as a negative control. ∗∗*P* < 0.01; ∗*P* < 0.05, calculated by Student's *t*-test. Data in (B), (G), (H) and (I) are shown as means ± SEM. For samples under copper stress, 500 μM copper sulfate was added into the medium for the final 12 h before collection. NT, normal condition; Cu, copper stress.

Hlc regulates basal but not stress-induced transcription

Based on the above observations, we speculated that Hlc may somehow regulate *MtnA* at the transcriptional level. To test the hypothesis, we monitored the transcription activity of *MtnA* by nuclear-run on (NRO) assays (Figure 1E, left panel), a classic method for examining the nascent transcript abundance of a gene of interest (42,43). The newly-generated *MtnA* transcript was purified with anti-BrUTP and analyzed by RT-qPCR with primer pairs detecting the 5′ end, middle or 3′ end of the precursor (Figure 1F). Compared to the treatment with the negative control (β-gal dsRNA), Hlc RNAi led to a ∼80% reduction in the abundance of the nascent *MtnA* transcript under normal conditions regardless of which primer pair was used (Figure 1G, higher panel), but had no effect under copper stress (Figure 1G, lower panel). The reference gene *U6* was also measured to minimize technological artifacts of each biological replicate under both conditions (Figure 1G). The *MtnA* precursor mRNA was highly enriched in NRO samples, excluding steady-state RNA contamination (Supplementary Figure S1B). Moreover, transcription inhibition assays, in which a 12 h transcription pulse of *MtnA* was triggered by addition of copper sulfate and turned off by Actinomycin D, demonstrated that neither knockdown nor overexpression of Hlc affected the half-life of *MtnA* mRNA (Supplementary Figure S2). This excludes the possibility that Hlc modulates the level of *MtnA* mRNA by enhancing its stability.

Given that *MtnA* is transcribed by RNA Pol II (8), we next investigated whether Hlc affects the density of Pol II at the locus of *MtnA* by ChIP experiments (Figure 1E, middle panel). Like the NRO assay, same primer pairs were used to measure the 5′ end, middle and 3′ end of the *MtnA* gene (Figure 1F). Following transfection with dsRNAs that target *Hlc*, the overall binding of Pol II to *MtnA* was significantly decreased under normal conditions (Figure 1H, higher panel), but had almost no change upon copper treatment (Figure 1H, lower panel). As a control, Pol II association of the house-keeping gene *Act42A* was not affected by Hlc knockdown under both conditions (Figure 1H).

In addition, we developed a rescue vector that only contains the coding region of *Hlc* and is insensitive to UTR dsRNA-mediated Hlc knockdown. As expected, rescue assays (Figure 1E, right panel) demonstrated that reexpression of Hlc significantly restored the level of *MtnA* mRNA under normal conditions (Figure 1I).

It is now known that circular RNAs are common outputs of many protein-coding genes via backsplicing (44–46). Therefore, we also investigated whether different splicing patterns influence Hlc-mediated transcription regulation using our previously described Hy_pMtnA dati Exons 1–3 vector (15,47), which is under control of the *MtnA* promoter and can produce a linear *dati* RNA as well as a circular version (Supplementary Figure S3A). Compared to the β-gal dsRNA control, both linear and circular *dati* RNA were significantly down-regulated upon Hlc knockdown under normal, but not stressed, conditions (Supplementary Figure S3B, C). These data suggest that (i) Hlc regulates basal transcription in a canonical splicing or backsplicing independent manner, and that (ii) Hlc-mediated

transcription regulation seems to rely on the context of the promoter region.

Collectively, these results strongly demonstrate that Hlc is specifically required for the basal transcription of the metal-responsive gene *MtnA* and indicate the essential role of Hlc in discrimination of basal and stress-induced transcription.

**Hlc directly targets the promoter and gene body of *MtnA***

Given that transcription is a tightly-controlled process that mainly occurs in the nucleus (48), we thus investigated whether the endogenous *Drosophila* Hlc is a nuclear protein by immunofluorescence staining assays and confocal microscopy analyses. As observed, Hlc was detected in both the nucleus and cytoplasm (Figure 2A, B). Relatively, ∼75% was present in the nuclear fraction and ∼25% was present in the cytoplasmic fraction (Figure 2C). Same experiments examining the subcellular localization of the FLAG-tagged Hlc confirmed the above phenotype (Supplementary Figure S4). Therefore, we concluded that Hlc translocates between the nucleus and cytoplasm and is primarily enriched in the nucleus.

To ask whether Hlc directly regulates the transcription of *MtnA*, we examined the density of Hlc at the locus of *MtnA* by ChIP experiments. Primer pairs spanning the promoter region and gene body of *MtnA* were used (Figure 2D). Compared to the negative IgG control, Hlc was found to interact with both the promoter region (0–400 bp upstream of the TSS) and gene body of *MtnA* under normal conditions (Figure 2E, left panel). Intriguingly, Hlc only exhibited a limited binding capacity towards *MtnA* in response to copper treatment (Figure 2E, left panel). No obvious interaction between Hlc and the house-keeping gene *Act5C* was observed, which further confirmed the specificity of Hlc-mediated regulation (Figure 2E, right panel). Moreover, the subcellular localization (Figure 2F, G) and protein level (Figure 2H, I) of Hlc were unaffected in copper-stressed cells. These results rule out the possibility that copper ions induce the disassociation of Hlc from *MtnA* by triggering Hlc nuclear export or affecting Hlc protein level.

The binding of Hlc to *MtnA* is required for the basal transcription of *MtnA*

To search the potential DNA binding domain of Hlc, we took advantage of DP-Bind (a web server for sequence-based prediction of DNA-binding sites) and found that amino acids 517–557 of Hlc had a potential DNA-binding capacity (49). In support, ChIP-qPCR experiments demonstrated that the interaction between Hlc and *MtnA* was drastically reduced upon deletion of the predicted DNA-binding domain (Supplementary Figure S5). This mutant was referred to ΔDBD herein.

Since thousands of studies have proved that protein–DNA interactions play a significant role in the transcription regulation of many eukaryotic genes (48,50,51), we next asked whether the direct interaction between Hlc and *MtnA* is essential to the accurate function of Hlc in the process of basal transcription. To this end, the vector expressing the ΔDBD mutant (Figure 3A) was introduced into the Hlc UTR dsRNA treated cells. The expression level of *MtnA*
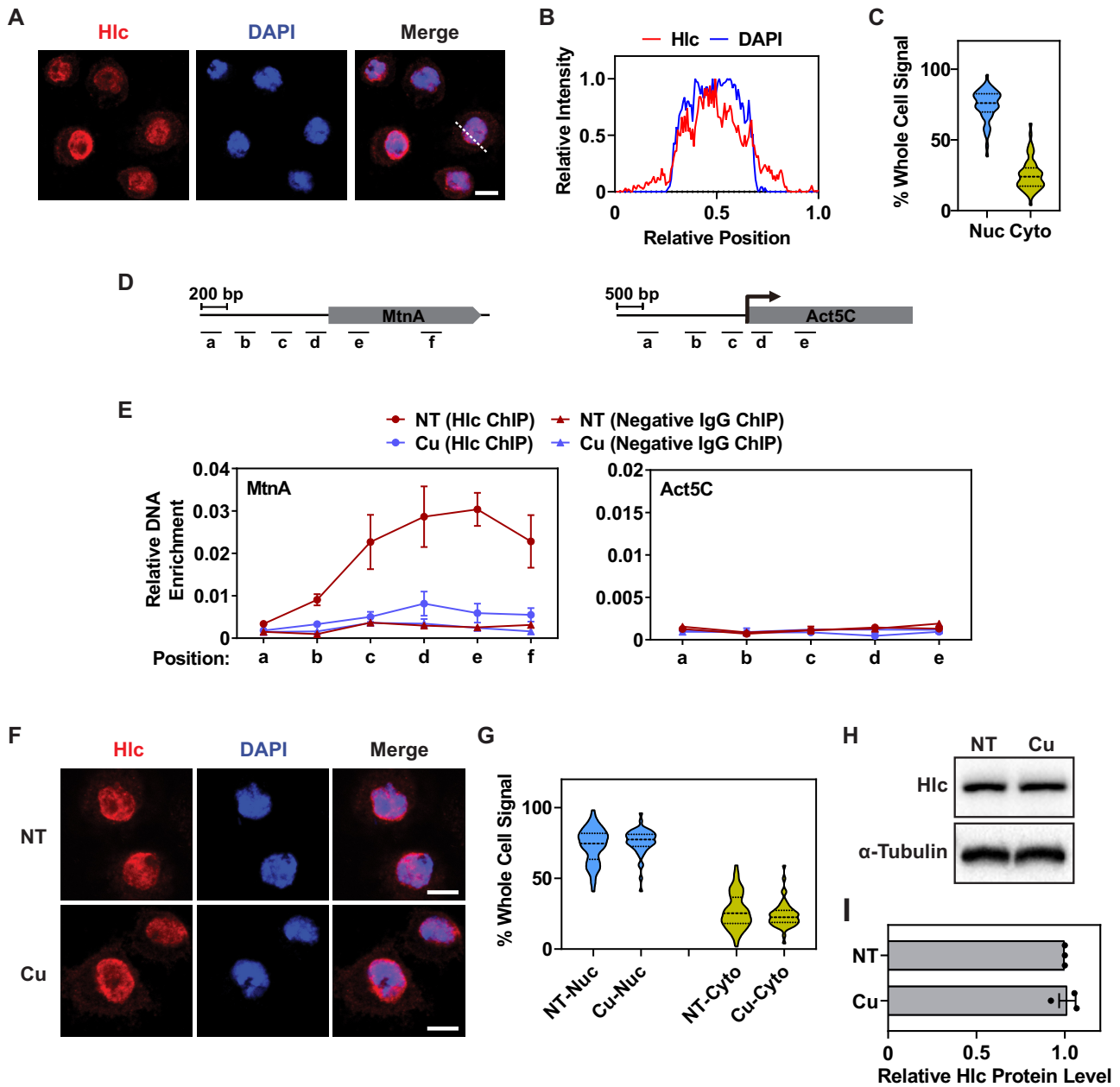
Figure 2. Hlc is a nuclear-localized protein and interacts with the genomic *MtnA*. (**A**) Confocal microscopy analysis of the endogenous Hlc immunofluorescence signals in S2 cells. Representative images from three biological replicates are shown. Scale bar = 5 μm. (**B**) Line profiles of both fluorescence intensities (Hlc and DAPI) along the dashed line, present in (A), confirming the nuclear localization of Hlc. (**C**) Violin plots reflecting the relative proportion of nuclear and cytoplasmic Hlc from the sample described in (A) (*n* = 50 cells for fluorescence signal quantification). Lines inside each violin plot represent the first quartile, median and third quartile of the data. (**D**) Schematic representations of the genomic *MtnA* and *Act5C* with the approximate locations of ChIP amplicons. (**E**) Hlc ChIP assay measuring the binding of Hlc to the genomic *MtnA* in cells treated with or without copper sulfate (*n* = 3 biological replicates). The reference gene *Act5C* served as a negative control. The negative IgG was used in each ChIP experiment to exclude artifacts of non-specific binding. The DNA binding sites of Hlc were defines as genomic regions enriched over the input DNA. Data are shown as means ± SEM. (**F**) Confocal microscopy analysis of the endogenous Hlc immunofluorescence signals in cells treated with or without copper sulfate. Representative images from three biological replicates are shown. Scale bar = 5 μm. (**G**) Violin plots reflecting the relative proportion of nuclear and cytoplasmic Hlc from samples described in (F) (*n* = 50 cells for fluorescence signal quantification per sample). Lines inside each violin plot represent the first quartile, median and third quartile of the data. (**H**) Western blots of the endogenous Hlc with protein extracts from cells treated with or without copper sulfate. α-Tubulin served as a loading control. (**I**) Bar chart showing the quantified protein level of Hlc from three independent blots (each replicate present as a black dot). Data were normalized to the unstressed sample and are shown as means ± SEM. For samples under copper stress, 500 μM copper sulfate was added into the medium for the final 12 h before collection. NT, normal condition; Cu, copper stress.
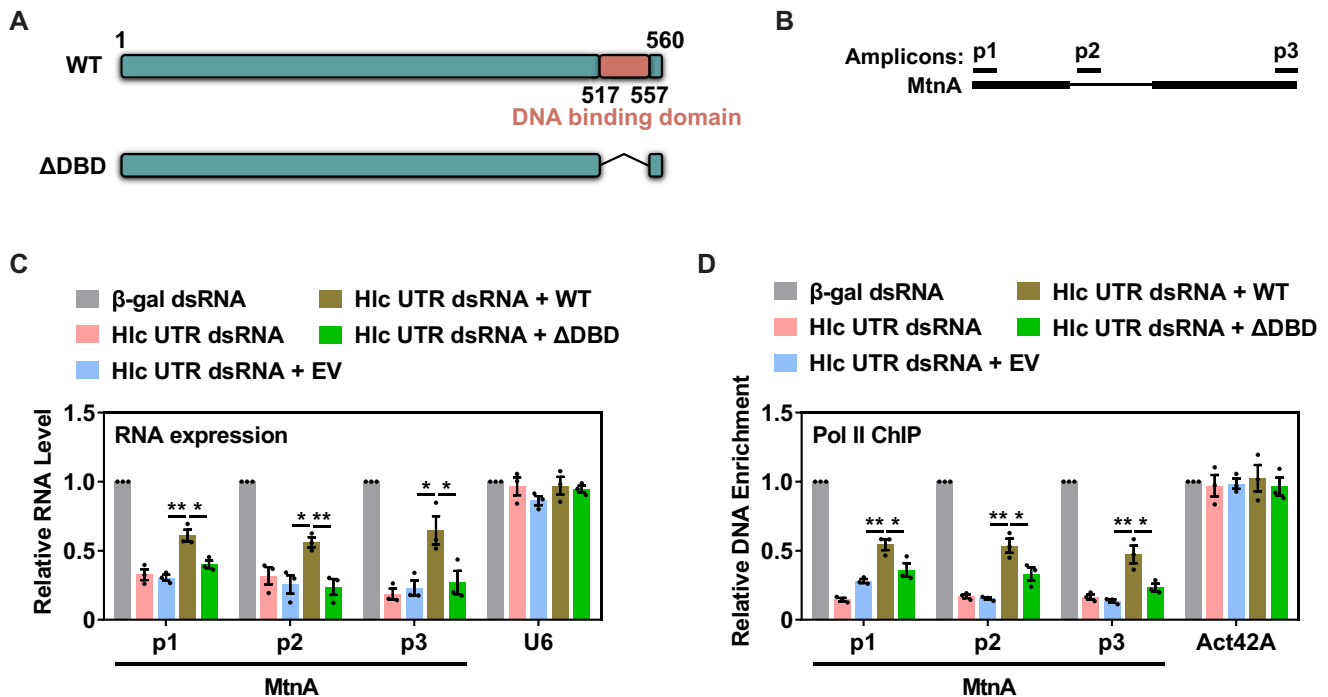
Figure 3. Hlc functions as a DNA binding protein. (**A**) Schematic representations of the wild-type Hlc (WT) and its ΔDBD mutant. The position of the DNA binding domain is marked in pink. (**B**) The approximate locations of primer pairs detecting the 5′ end, middle or 3′ end of the *MtnA* gene body. (**C**) RT-qPCR quantification of *MtnA* expression using whole-cell RNA extracts purified from the control RNAi, Hlc RNAi, empty vector control rescued, WT Hlc vector rescued or ΔDBD Hlc vector rescued cells ($n = 3$ biological replicates; each replicate present as a black dot). The reference gene *U6* served as a negative control. $**P < 0.01$; $*P < 0.05$, calculated by Student's *t*-test. (**D**) Pol II ChIP assay measuring Pol II density at the locus of *MtnA* after the same knockdown-rescue experiment as described in Figure 3C ($n = 3$ biological replicates; each replicate present as a black dot). The reference gene *Act42A* served as a negative control. $**P < 0.01$; $*P < 0.05$, calculated by Student's *t*-test. Data in (C) and (D) are shown as means ± SEM.

and the occupancy of Pol II were measured with primer pairs detecting the 5′ end, middle or 3′ end of the *MtnA* gene body (Figure 3B–D). Different from the wild-type Hlc, the ΔDBD mutant failed to restore *MtnA* expression (Figure 3C) or Pol II density at the *MtnA* locus (Figure 3D), confirming the contribution of the DNA binding domain of Hlc in promoting *MtnA* transcription under normal conditions. Recall that Hlc was released from the *MtnA* locus in response to copper treatment (Figure 2E, left panel), which can explain the specificity of Hlc-mediated regulation in basal transcription.

Hlc functions in a gawky-independent manner

In contrast to Hlc, it was recently demonstrated that *Drosophila* gawky is only required for metal stress-induced transcription activation but is bypassed from basal transcription (15). In addition, the binding capacity of gawky towards the promoter of *MtnA* was robustly elevated under metal stress (15). Therefore, we asked whether gawky affects the interaction between Hlc and *MtnA* during the transition from the basal to copper-induced transcription. To this end, we performed Hlc ChIP experiments using gawky RNAi cells treated with or without copper. As observed, the binding of Hlc to *MtnA* was not affected by gawky knockdown under normal conditions (Figure 4A), supporting that gawky is not involved in Hlc-mediated basal transcription regulation. Surprisingly, gawky knockdown resulted in

an elevated interaction between Hlc and *MtnA* under copper stress (Figure 4B). This can be explained by the assumption that Hlc rebound to *MtnA* to sustain its basal transcription after the metal-induced transcription had been impaired.

Next, we performed gawky ChIP experiments and found that knockdown of Hlc had almost no effect on the binding of gawky to *MtnA*, indicating that Hlc is dispensable for gawky-mediated transcription activation (Supplementary Figure S6). As a control, the house-keeping gene *Act5C* exhibited no changes in Hlc or gawky ChIP signals in above experiments (Figure 4; Supplementary Figure S6). Taken together, these results support that Hlc specifically controls basal transcription while gawky specifically regulates metal-induced transcription.

Hlc enhances the genomic accessibility around the TSS of *MtnA*

The compaction of genomic DNA into chromatin has a fundamental role in the transcription regulation of many genes (52–54). Emerging studies have demonstrated that a group of DEAD-box helicases (e.g. DDX5 and DDX17) are able to modulate nucleosome compaction, chromatin organization and the accessibility of DNA into chromatin in an active or repressive way (55–59). Informed by these findings as well as our data present in Figure 1, we reasoned that Hlc may maintain the transcription activity of *MtnA* through
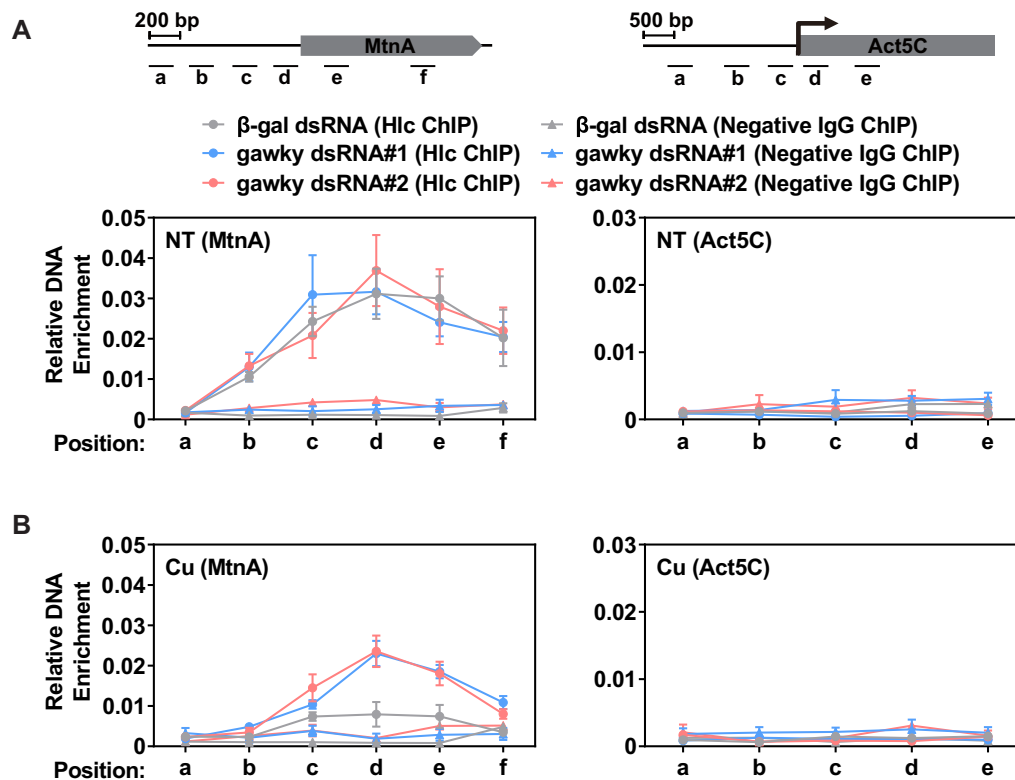
Figure 4. Hlc functions in a gawky-independent manner. (**A**, **B**) Hlc ChIP assay measuring the binding of Hlc to the genomic *MtnA* after cells had been individually treated with two independent gawky dsRNAs ($n = 3$ biological replicates). The reference gene *Act5C* served as a negative control. The negative IgG was used to exclude artifacts of non-specific binding. The DNA binding sites of Hlc were defines as genomic regions enriched over the input DNA. Schematic representations of the genomic *MtnA* and *Act5C* with the approximate locations of ChIP amplicons are shown on top. Data are shown as means ± SEM. For samples under copper stress, 500 μM copper sulfate was added into the medium for the final 12 h before collection. NT, normal condition; Cu, copper stress.

regulating chromatin organization. To test this hypothesis, we measured the accessibility of the genomic region surrounding the *MtnA* TSS by MNase protection assays (Figure 5A), a classic method used to profile the active chromatin region of a gene of interest (60,61). Limited digestion of chromatin with the endo- and exo-nuclease MNase cleaves the exposed DNA between adjacent nucleosomes, but significantly enriches the genomic DNA fragments that are wrapped around histone octamers (60,61). As expected, agarose gel electrophoresis showed that mononucleosome-protected DNA fragments (∼150 bp) were released by MNase cleavage from chromatin isolated from β-gal (the RNAi control) and Hlc RNAi cells (Figure 5B). Subsequent qPCR analysis was performed with seven overlapping amplicons to tile through the genomic region surrounding the *MtnA* TSS (–250 to +257 bp) and quantify the digestion extent of MNase treatment (Figure 5B). The relative protection level was defined as the ratio of MNase-digested to undigested genomic DNA. Compared to the β-gal dsRNA control (set to '1'), knockdown of Hlc resulted in a significant increase in the MNase protection level at the genomic region spanning from –84 to +257 bp relative to the TSS (Figure 5C), suggesting the formation of a closed/inactive chromatin architecture near the TSS. Taken together, the result supports a model in which Hlc maintains an open chromatin architecture near the TSS of *MtnA* to allow loading

of the general transcriptional machinery (e.g. Pol II) for the basal transcription of *MtnA*.

The helicase ATP binding domain of Hlc is required for open chromatin maintenance

Considering that helicases are a class of ubiquitous and highly-conserved regulators that function in the structure modulation of double-stranded nucleic acids in an energy-dependent manner (16–18), we thus asked whether the helicase ATP binding domain of Hlc contributes to open chromatin maintenance. To fill the gap, we constructed a vector which can express an RNAi-resistant Hlc mutant deleted of the helicase ATP binding domain (referred to ΔHD herein) (Figure 6A). The control, wild-type and ΔHD vector were individually introduced into the Hlc UTR dsRNA treated cells, and MNase protection experiments were performed to measure the chromatin architecture at the *MtnA* TSS. Distinct from what was observed with the wild-type Hlc, reexpression of the ΔHD mutant failed to eliminate the closed chromatin architecture, but instead slightly increased the MNase protection level at the *MtnA* TSS relative to the Hlc knockdown sample (Figure 6B). This phenotype suggests that the ΔHD mutant can function like a dominant-negative protein. Indeed, loss of the helicase ATP binding domain did not affect the interac-
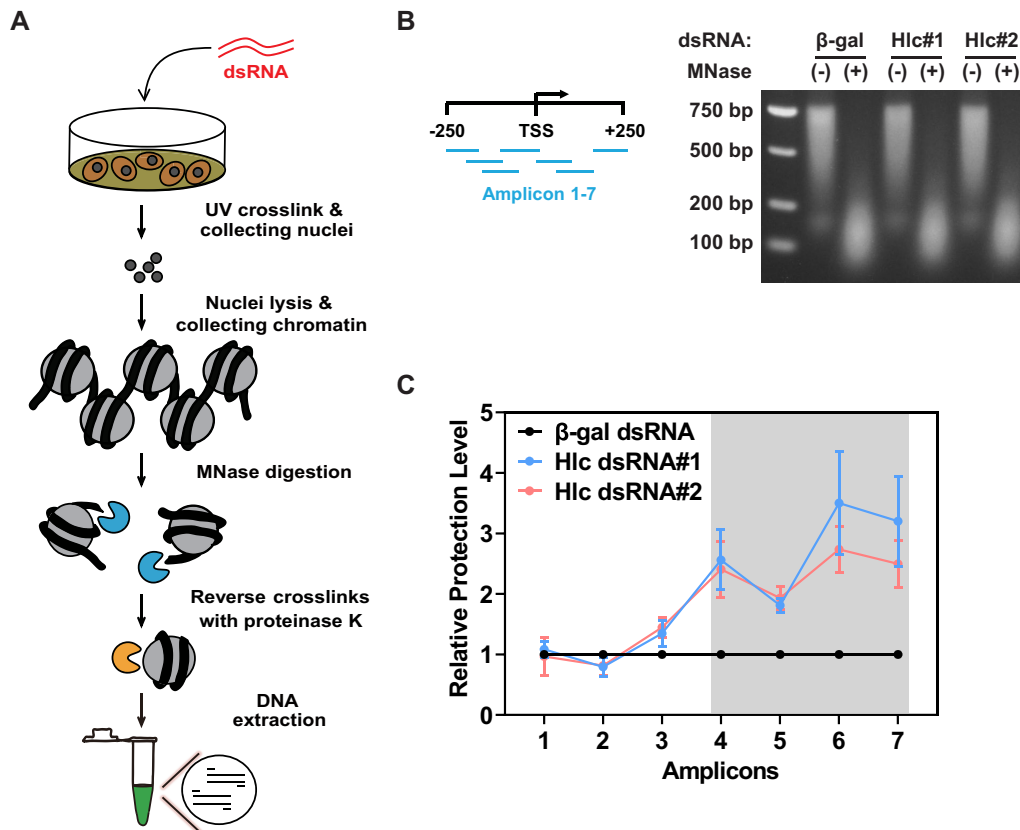
Figure 5. Hlc is required for chromatin opening near the TSS of *MtnA*. (**A**) A schematic overview of the experimental setup for the MNase protection assay. (**B**) Left, the approximate locations of seven overlapping qPCR amplicons spanning the *MtnA* TSS. These amplicons were used to measure the MNase protection level at each position. Right, agarose gel electrophoresis verifying that mononucleosome-protected DNA fragments were released by MNase digestion. (**C**) MNase protection analysis in the control (β-gal) or Hlc RNAi cells (*n* = 3 biological replicates). The relative protection level was defined as the ratio of MNase-digested to undigested genomic DNA. To better reflect the effect of Hlc knockdown on chromatin opening, the β-gal dsRNA control was set to '1' at each examined site. Data are shown as means ± SEM. Statistically significant differences between the control and Hlc RNAi samples ($P < 0.05$, calculated by Student's *t*-test), if any, are marked with the grey box.

tion between Hlc and *MtnA* (Supplementary Figure S7A) or the nuclear-cytoplasmic distribution of Hlc (Supplementary Figure S7B, C).

To further examine whether the helicase ATP binding domain of Hlc regulates the basal transcription of *MtnA*, we quantified the level of *MtnA* mRNA and the density of Pol II after rescue experiments same to what was described in Figure 6B. Consistently, the ΔHD mutant failed to restore *MtnA* expression (Figure 6C) or Pol II occupancy at the *MtnA* locus (Figure 6D). Taken together, we concluded that the proper activity of Hlc in open chromatin maintenance and *MtnA* transcription depends on its helicase ATP binding domain.

Hlc plays a widespread and potent role in the basal transcription of a subset of *Drosophila* stress-responsive genes

In order to substantiate the importance of Hlc-mediated transcription regulation, we thus asked whether additional stress-responsive genes are similarly regulated in *Drosophila*. To this end, two independent dsRNAs against *Hlc* (#2 and 3) were used to knockdown Hlc expression in unstressed S2 cells and RNA-seq was subsequently per-

formed to measure global gene expression. As observed, out of 1983 differentially expressed protein-coding genes, 1101 were significantly down-regulated upon treatment with Hlc dsRNA#2 (fold change (log$_2$) >1 and $P < 0.001$) (Figure 7A). Gene ontology analysis indicated that the set of down-regulated genes was enriched for the category related to 'response to stress' (Figure 7B). Notably, stress-responsive genes were more sensitive to Hlc knockdown among these down-regulated genes, since loss of Hlc reduced the expression level of stress-responsive genes to a greater extent than that of non-stress genes (Figure 7C). In particular, a number of *Hsp* mRNAs were identified among the most down-regulated genes (Figure 7D). For example, the basal transcription of *Hsp23* and *Hsp26* was almost completely silent upon Hlc knockdown (Figure 7E, F). Moreover, we utilized the previously published ATAC-seq (a high-throughput method for mapping global chromatin accessibility) dataset (38) and found that down-regulated stress-responsive genes had a more accessible chromatin structure around their TSSs relative to unchanged stress-responsive genes (Figure 7G). Consistently, similar phenotypes were observed with the Hlc dsRNA#3 sample (Supplementary Figure S8). These results support
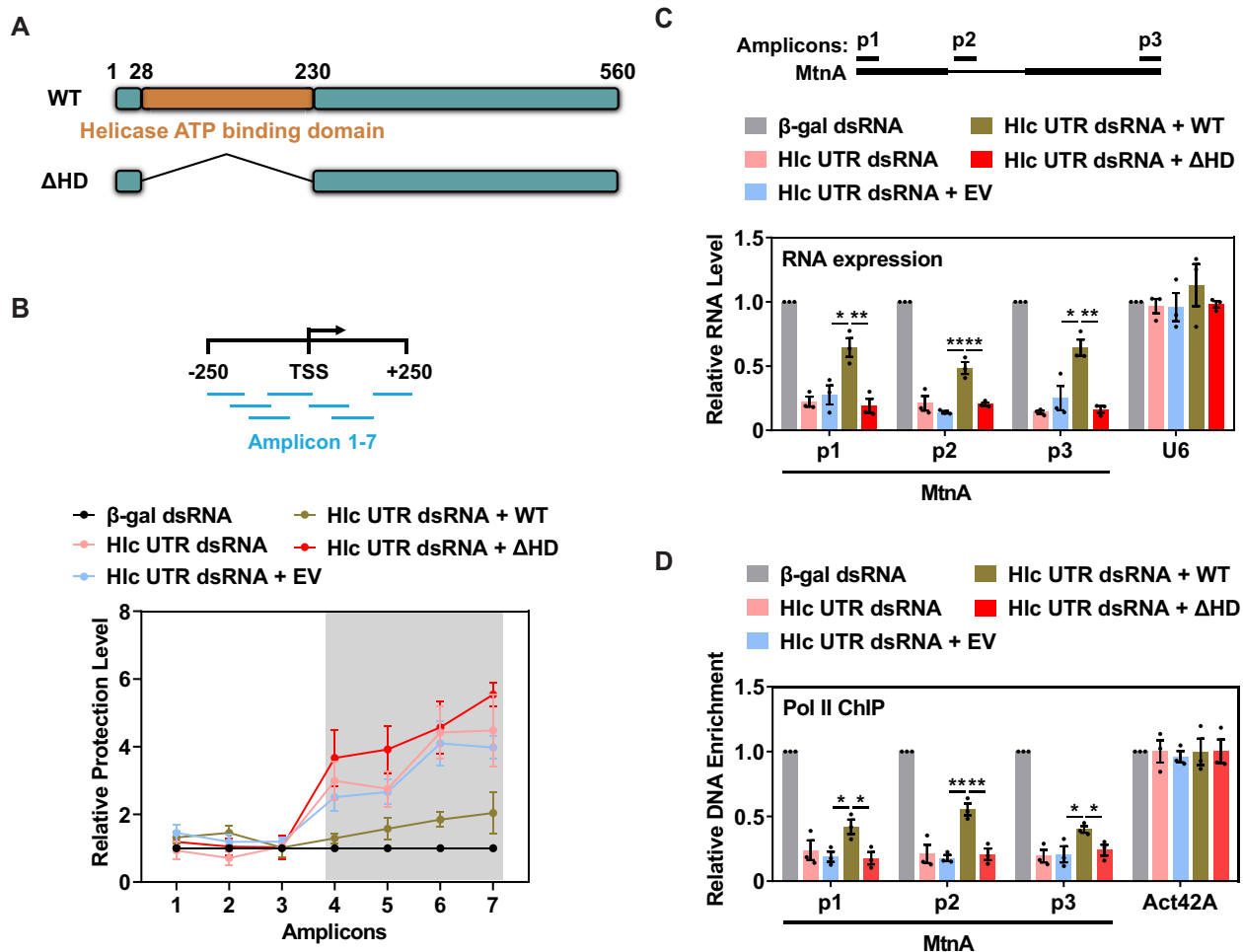
Figure 6. The helicase ATP binding domain of Hlc is required for chromatin opening. (**A**) Schematic representations of the wild-type Hlc (WT) and its ΔHD mutant. The position of the helicase ATP binding domain is marked in orange. (**B**) MNase protection analysis in the control RNAi, Hlc RNAi, empty vector control rescued, WT Hlc vector rescued or ΔHD Hlc vector rescued cells ($n = 3$ biological replicates). The relative protection level was defined as the ratio of MNase-digested to undigested genomic DNA. The β-gal dsRNA control was set to '1' at each examined site. Statistically significant differences between the WT and ΔHD Hlc vector rescued samples ($P < 0.05$, calculated by Student's t-test), if any, are marked with the grey box. The approximate locations of seven overlapping qPCR amplicons spanning the *MtnA* TSS are shown on top. (**C**) RT-qPCR quantification of *MtnA* expression after the same knockdown-rescue experiment as described in (B) ($n = 3$ biological replicates; each replicate present as a black dot). The approximate locations of primer pairs detecting the 5′ end, middle or 3′ end of the *MtnA* gene body are shown on top. The reference gene *U6* served as a negative control. ∗∗$P < 0.01$; ∗$P < 0.05$, calculated by Student's t-test. (**D**) Pol II ChIP assay measuring Pol II density at the locus of *MtnA* with primer pairs shown in (C) after the same knockdown-rescue experiment as described in (B) and (C) ($n = 3$ biological replicates; each replicate present as a black dot). The reference gene *Act42A* served as a negative control. ∗∗$P < 0.01$; ∗$P < 0.05$, calculated by Student's t-test. Data in Figure 6B–D are shown as means ± SEM.

the function of Hlc in the basal transcription and open chromatin maintenance of a subset of stress-responsive genes.

Based on the above observation (Figure 7D–F), we next focused on *Hsps* to validate our RNA-seq result. As expected, RT-qPCR analysis demonstrated that knockdown of Hlc led to a significant and robust reduction in the basal, but not heat shock-induced, transcription of all *Hsp* mRNAs examined (Figure 7H), analogous to our prior results with *MtnA*. Taken together, we concluded that Hlc-mediated transcription regulation represents a general mechanism for cells to specifically regulate the basal transcription of a subset of stress-responsive genes in *Drosophila*.

DISCUSSION

Significant transcription reprogramming occurs to help cells establish multiple adaptive responses in the presence of stressed conditions (1,2). Typically, the transcription activity returns to its basal level after the stress has been removed (1,2). Despite employing the same transcription machinery (e.g. Pol II), cells may use different pathways to dictate basal and stress-induced transcription states. Based on the hypothesis, we aimed to search regulators that function exclusively in each transcription state. As expected, our previous study has identified gawky as a metal stress 'checkpoint', which specifically activates metal-induced transcription by promoting MTF-1 nuclear import and recruiting MTF-1 to the promoter of metal-responsive genes (15).
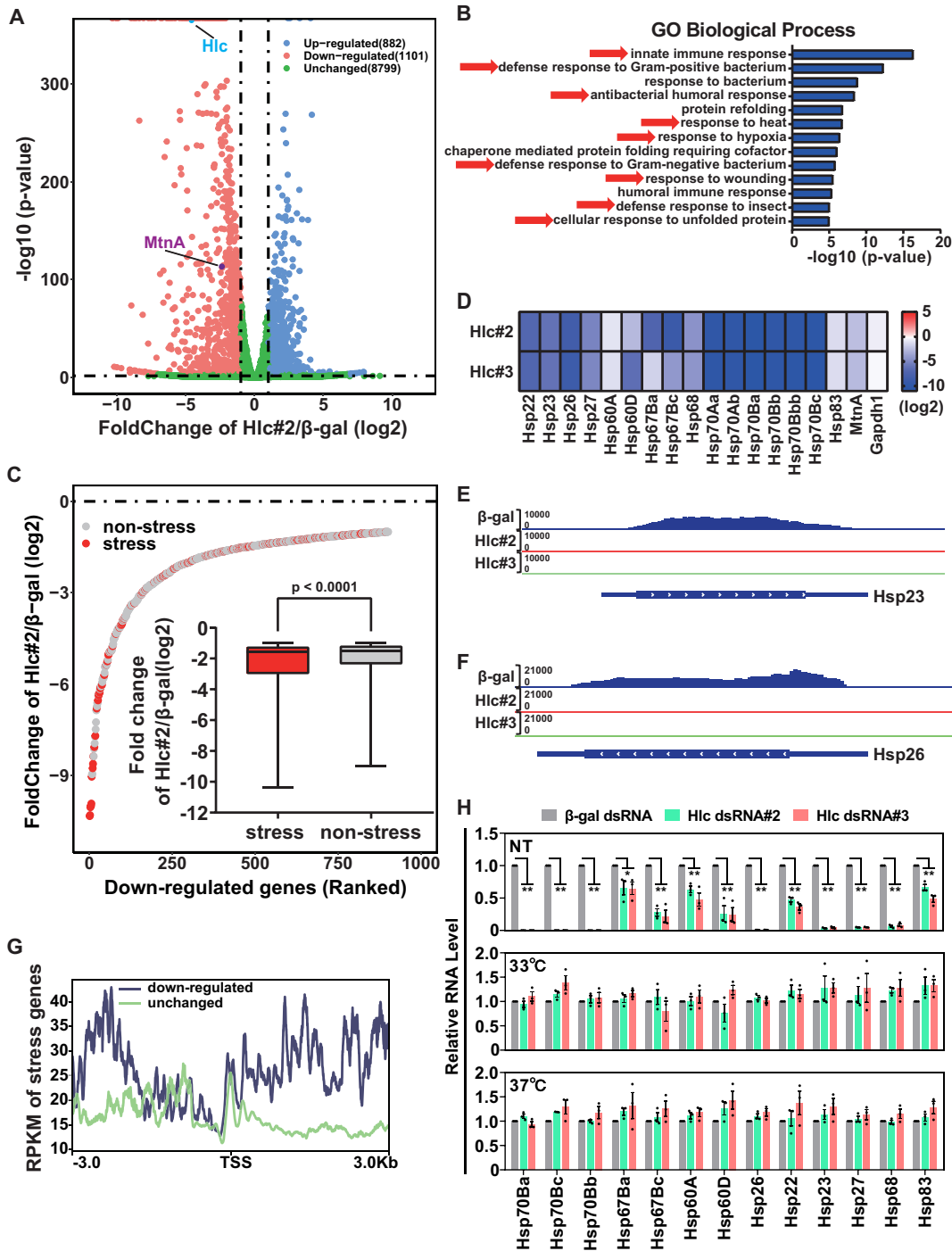
Figure 7. Hlc plays a general role in the basal transcription of *Drosophila* stress-responsive genes. (**A**) Volcano plot showing differentially expressed protein-coding genes in *Drosophila* S2 cells treated with Hlc dsRNAs (#2). *MtnA* is present as a purple dot and *Hlc* is present as a light blue dot. Threshold used to define Hlc-regulated genes is fold change ($\log_2$) > 1 and $P < 0.001$. *P* value is calculated by Wald chi-squared test. For each gene selected in following analyses (B, C and G), combined reads from the control and Hlc RNAi (#2) samples are ≥1000. (**B**) Gene ontology (GO) analysis identifying categories of genes that are enriched among down-regulated genes. Note that subcategories with red arrows belong to the main category 'response to stress' (GO:0006950). Subcategories are ranked by their statistical significance, and *P* value is calculated by Fisher's exact test. (**C**) Rank-ordered plot reflecting the fold change of down-regulated genes. Genes are ranked by their fold change, and stress-responsive genes are highlighted as red dots. A boxplot comparing the reduction extent between stress-responsive and non-stress genes is also shown in the middle. *P* value is calculated by Student's *t*-test. (**D**) Heat map highlighting the fold change of *Hsp* genes upon Hlc knockdown. *MtnA* served as a positive control and *Gapdh1* served as a negative control. (**E, F**) Integrative Genomics Viewer (IGV) snapshot of *Hsp23* and *Hsp26* expression in the control and Hlc RNAi cells. (**G**) Density plot reflecting ATAC-seq normalized signals around TSSs of down-regulated (blue line) or unchanged (green line) stress-responsive genes in the RNA-seq dataset. (**H**) RT-qPCR quantification of *Hsp* expression using whole-cell RNA extracts purified from the control and Hlc RNAi cells. To activate heat shock-induced transcription, cells were cultured at 33 or 37°C for the final 1 h before collection. ∗∗$P < 0.01$; ∗$P < 0.05$, calculated by Student's t-test. Data are shown as means ± SEM. NT, normal condition; 33 and 37°C, heat stress.
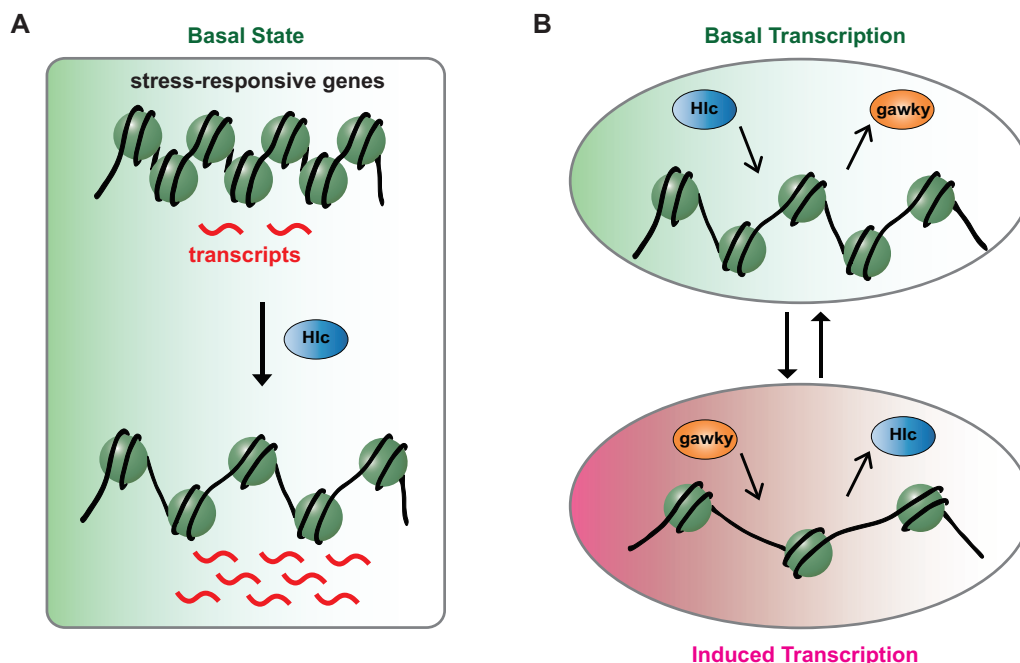
Figure 8. A working model for Hlc-mediated transcription regulation. (**A**) Hlc ensures the basal transcription of stress-responsive genes by maintaining an open and accessible chromatin structure. (**B**) In the case of transition between normal and metal-stressed conditions, Hlc specifically regulates basal transcription while gawky specifically regulates induced transcription.

Here, this study proposes that the DEAD-box helicase Hlc specifically regulates the basal transcription of a subgroup of stress-responsive genes but is dispensable for their induced transcription. The focused investigation regarding *MtnA* highlights the molecular mechanism of Hlc-mediated transcription regulation: Hlc binds to the genomic locus of *MtnA* to increase its DNA accessibility by maintaining an open chromatin architecture, which ultimately allows assembly of the general transcriptional machinery (Figure 8A). Taken together, these studies propose that the changes in mechanisms of gene expression and transcription regulation are accompanied by changes in the chromatin environment which is modified by the binding of different *trans*-activators. At least in the case of metal stress, Hlc and gawky serve as essential factors to dictate basal and stress-induced transcription, respectively (Figure 8B).

Although it was long thought that Hlc functions as an RNA binding protein (19,20,23), our study suggests that Hlc also possesses a DNA binding capacity (Figure 2E). In addition, the binding of Hlc to DNA loci is indispensable for its proper function in basal transcription, as supported by the phenotype that (i) Hlc was almost completely disassociated from the *MtnA* locus in the presence of overloaded copper (Figure 2E) and that (ii) the ΔDBD mutant did not restore *MtnA* expression or Pol II recruitment in the Hlc UTR dsRNA treated cells (Figure 3C, D). We also noticed that Hlc rebound to the *MtnA* locus when copper-induced transcription was impaired by gawky knockdown (Figure 4B), recall that the binding of gawky to the *MtnA* locus is in a metal-dependent manner (15). These results further confirm that Hlc and gawky function anticooperatively on chromatin (Figure 8B).

The DEAD-box family modulates gene expression by controlling various aspects of RNA metabolism, such as

splicing, nuclear export and degradation (16–18). DDX5 is required for appropriate splicing of genes necessary for spermatogenesis (62). UAP56/DDX39B, as a component of the exon-junction complex, binds to nascent transcripts during splicing and recruits the export factor ALY to facilitate the nuclear export of bulk mRNAs (63–65). DDX6 destabilizes transcripts of differentiation-relevant genes through association with mRNA degradation factors (66). However, we found that knockdown of Hlc did not affect the splicing pattern (Supplementary Figure S3), subcellular distribution (Figure 1C) or stability (Supplementary Figure S2) of examined mRNAs. These results somehow exclude the possibility that Hlc may also function post-transcriptionally, at least for the regulation of *MtnA* expression. In addition, it is worth noting that nuclear quality control (i.e. RNA nuclear surveillance, a process to degrade incorrectly processed nascent transcripts in the nucleus (67–69)) can be bypassed for *Hsp* mRNAs only in response to heat hock (70), reminiscent of the phenotype of Hlc knockdown under stressed conditions. In this regard, we noticed that Hlc was not involved in premature transcription termination (Figure 1G, H). Therefore, it is not likely that Hlc co-transcriptionally affects steps of mRNA nuclear quality control. However, further investigation about this hypothesis is required.

Chromatin opening is a prerequisite for transcription. In this study, we found that Hlc is indispensable for open chromatin maintenance in the basal transcription state (Figure 5) and its helicase ATP binding domain contributes to this process (Figure 6). These data raise a hypothesis that Hlc acts as a direct functional enzyme to remodel chromatin and increase the accessibility of DNA. However, we cannot rule out the possibility that Hlc indirectly affects 3D chromatin organization through regulating the functional activity of

chromatin remodeling factors and/or affecting genome stability. In fact, DDX5 and DDX17 have been demonstrated to regulate histone modifications in association with different histone acetyltransferases and deacetylases in a context-specific manner (55–57). Moreover, UAP56/DDX39B has been found to interact with active chromatin and unwinds harmful RNA-DNA hybrids (71), a structure which is very likely formed by nuclear-retained linear and circular RNAs (47,64). Therefore, more effort is needed to clarify the detailed mechanism of Hlc-mediated chromatin opening, which is under way in our lab.

DATA AVAILABILITY

RNA-seq data were deposited in the Gene Expression Omnibus (GEO) repository (GSE205804) of NCBI.

SUPPLEMENTARY DATA

Supplementary Data are available at NAR Online.

ACKNOWLEDGEMENTS

FUNDING

REFERENCES

1. Vihervaara,A., Duarte,F.M. and Lis,J.T. (2018) Molecular mechanisms driving transcriptional stress responses. *Nat. Rev. Genet.*, **19**, 385–397.
2. de Nadal,E., Ammerer,G. and Posas,F. (2011) Controlling gene expression in response to stress. *Nat. Rev. Genet.*, **12**, 833–845.
3. Lynes,M.A., Kang,Y.J., Sensi,S.L., Perdrizet,G.A. and Hightower,L.E. (2007) Heavy metal ions in normal physiology, toxic stress, and cytoprotection. *Ann. N. Y. Acad. Sci.*, **1113**, 159–172.
4. Burke,R. (2022) Molecular physiology of copper in drosophila melanogaster. *Curr. Opin. Insect Sci.*, **51**, 100892.
5. Tang,D., Khaleque,M.A., Jones,E.L., Theriault,J.R., Li,C., Wong,W.H., Stevenson,M.A. and Calderwood,S.K. (2005) Expression of heat shock proteins and heat shock protein messenger ribonucleic acid in human prostate carcinoma in vitro and in tumors in vivo. *Cell Stress Chaperones*, **10**, 46–58.
6. Xiao,X., Zuo,X., Davis,A.A., McMillan,D.R., Curry,B.B., Richardson,J.A. and Benjamin,I.J. (1999) HSF1 is required for extra-embryonic development, postnatal growth and protection during inflammatory responses in mice. *EMBO J.*, **18**, 5943–5952.
7. Sims,H.I., Chirn,G.W. and Marr,M.T. 2nd (2012) Single nucleotide in the MTF-1 binding site can determine metal-specific transcription activation. *Proc. Natl. Acad. Sci. U.S.A.*, **109**, 16516–16521.
8. Tatomer,D.C., Elrod,N.D., Liang,D., Xiao,M.S., Jiang,J.Z., Jonathan,M., Huang,K.L., Wagner,E.J., Cherry,S. and Wilusz,J.E. (2019) The integrator complex cleaves nascent mRNAs to attenuate transcription. *Genes Dev.*, **33**, 1525–1538.
9. Krone,P.H., Evans,T.G. and Blechinger,S.R. (2003) Heat shock gene expression and function during zebrafish embryogenesis. *Semin. Cell Dev. Biol.*, **14**, 267–274.
10. Stetler,R.A., Gan,Y., Zhang,W., Liou,A.K., Gao,Y., Cao,G. and Chen,J. (2010) Heat shock proteins: cellular and molecular mechanisms in the central nervous system. *Prog. Neurobiol.*, **92**, 184–211.
11. Heuchel,R., Radtke,F., Georgiev,O., Stark,G., Aguet,M. and Schaffner,W. (1994) The transcription factor MTF-1 is essential for basal and heavy metal-induced metallothionein gene expression. *EMBO J.*, **13**, 2870–2875.
12. Gunther,V., Lindert,U. and Schaffner,W. (2012) The taste of heavy metals: gene regulation by MTF-1. *Biochim. Biophys. Acta*, **1823**, 1416–1425.
13. Selvaraj,A., Balamurugan,K., Yepiskoposyan,H., Zhou,H., Egli,D., Georgiev,O., Thiele,D.J. and Schaffner,W. (2005) Metal-responsive transcription factor (MTF-1) handles both extremes, copper load and copper starvation, by activating different genes. *Genes Dev.*, **19**, 891–896.
14. Marr,M.T., Isogai,Y., Wright,K.J. and Tjian,R. (2006) Coactivator cross-talk specifies transcriptional output. *Genes Dev.*, **20**, 1458–1469.
15. Jia,R., Song,Z., Lin,J., Li,Z., Shan,G. and Huang,C. (2021) Gawky modulates MTF-1-mediated transcription activation and metal discrimination. *Nucleic. Acids. Res.*, **49**, 6296–6314.
16. Linder,P. and Jankowsky,E. (2011) From unwinding to clamping - the DEAD box RNA helicase family. *Nat. Rev. Mol. Cell Biol.*, **12**, 505–516.
17. Sergeeva,O. and Zatsepin,T. (2021) RNA helicases as shadow modulators of cell cycle progression. *Int. J. Mol. Sci.*, **22**, 2984.
18. Jankowsky,E. (2011) RNA helicases at work: binding and rearranging. *Trends Biochem. Sci*, **36**, 19–29.
19. Zirwes,R.F., Eilbracht,J., Kneissel,S. and Schmidt-Zachmann,M.S. (2000) A novel helicase-type protein in the nucleolus: protein NOH61. *Mol. Biol. Cell*, **11**, 1153–1167.
20. Daugeron,M.C., Kressler,D. and Linder,P. (2001) Dbp9p, a putative ATP-dependent RNA helicase involved in 60S-ribosomal-subunit biogenesis, functionally interacts with dbp6p. *RNA*, **7**, 1317–1334.
21. Pryszlak,M., Wiggans,M., Chen,X., Jaramillo,J.E., Burns,S.E., Richards,L.M., Pugh,T.J., Kaplan,D.R., Huang,X., Dirks,P.B. *et al.* (2021) The DEAD-box helicase DDX56 is a conserved stemness regulator in normal and cancer stem cells. *Cell Rep.*, **34**, 108903.
22. Xu,Z., Anderson,R. and Hobman,T.C. (2011) The capsid-binding nucleolar helicase DDX56 is important for infectivity of west nile virus. *J. Virol.*, **85**, 5571–5580.
23. Taschuk,F., Tapescu,I., Moy,R.H. and Cherry,S. (2020) DDX56 binds to chikungunya virus RNA to control infection. *Mbio*, **11**, e02623-20.
24. Pirincal,A. and Turan,K. (2021) Human DDX56 protein interacts with influenza a virus NS1 protein and stimulates the virus replication. *Genet Mol Biol*, **44**, e20200158.
25. Fu,S.Z., Yang,W.P., Ru,Y., Zhang,K.S., Wang,Y., Liu,X.T., Li,D. and Zheng,H.X. (2019) DDX56 cooperates with FMDV 3A to enhance FMDV replication by inhibiting the phosphorylation of IRF3. *Cell Signal*, **64**, 109393.
26. Kouyama,Y., Masuda,T., Fujii,A., Ogawa,Y., Sato,K., Tobo,T., Wakiyama,H., Yoshikawa,Y., Noda,M., Tsuruda,Y. *et al.* (2019) Oncogenic splicing abnormalities induced by DEAD-Box helicase 56 amplification in colorectal cancer. *Cancer Sci.*, **110**, 3132–3144.
27. Wu,Q., Luo,X., Terp,M.G., Li,Q., Li,Y., Shen,L., Chen,Y., Jacobsen,K., Bivona,T.G., Chen,H. *et al.* (2021) DDX56 modulates post-transcriptional wnt signaling through miRNAs and is associated with early recurrence in squamous cell lung carcinoma. *Mol. Cancer*, **20**, 108.

28. Cui,Y., Hunt,A., Li,Z., Birkin,E., Lane,J., Ruge,F. and Jiang,W.G. (2021) Lead DEAD/H box helicase biomarkers with the therapeutic potential identified by integrated bioinformatic approaches in lung cancer. *Comput. Struct. Biotechnol. J.*, **19**, 261–278.

29. Song,Z., Jia,R., Tang,M., Xia,F., Xu,H., Li,Z. and Huang,C. (2021) Antisense oligonucleotide technology can be used to investigate a circular but not linear RNA-mediated function for its encoded gene locus. *Sci. China Life Sci.*, **64**, 784–794.

30. You,J., Song,Z., Lin,J., Jia,R., Xia,F., Li,Z. and Huang,C. (2021) RNAi-directed knockdown induces nascent transcript degradation and premature transcription termination in the nucleus. *Cell Discov.*, **7**, 79.

31. Jia,R., Xiao,M.S., Li,Z., Shan,G. and Huang,C. (2019) Defining an evolutionarily conserved role of GW182 in circular RNA degradation. *Cell Discov.*, **5**, 45.

32. Bolger,A.M., Lohse,M. and Usadel,B. (2014) Trimmomatic: a flexible trimmer for illumina sequence data. *Bioinformatics*, **30**, 2114–2120.

33. Aken,B.L., Ayling,S., Barrell,D., Clarke,L., Curwen,V., Fairley,S., Fernandez Banet,J., Billis,K., Garcia Giron,C., Hourlier,T. *et al.* (2016) The ensembl gene annotation system. *Database (Oxford)*, **2016**, baw093.

34. Trapnell,C., Pachter,L. and Salzberg,S.L. (2009) TopHat: discovering splice junctions with RNA-Seq. *Bioinformatics*, **25**, 1105–1111.

35. Pertea,M., Pertea,G.M., Antonescu,C.M., Chang,T.C., Mendell,J.T. and Salzberg,S.L. (2015) StringTie enables improved reconstruction of a transcriptome from RNA-seq reads. *Nat. Biotechnol.*, **33**, 290–295.

36. Love,M.I., Huber,W. and Anders,S. (2014) Moderated estimation of fold change and dispersion for RNA-seq data with DESeq2. *Genome Biol.*, **15**, 550.

37. Sherman,B.T., Hao,M., Qiu,J., Jiao,X., Baseler,M.W., Lane,H.C., Imamichi,T. and Chang,W. (2022) DAVID: a web server for functional enrichment analysis and functional annotation of gene lists (2021 update). *Nucleic Acids Res.*, **50**, W216–W221.

38. Merrill,C.B., Montgomery,A.B., Pabon,M.A., Shabalin,A.A., Rodan,A.R. and Rothenfluh,A. (2022) Harnessing changes in open chromatin determined by ATAC-seq to generate insulin-responsive reporter constructs. *BMC Genomics*, **23**, 399.

39. Tarasov,A., Vilella,A.J., Cuppen,E., Nijman,I.J. and Prins,P. (2015) Sambamba: fast processing of NGS alignment formats. *Bioinformatics*, **31**, 2032–2034.

40. Ramirez,F., Dundar,F., Diehl,S., Gruning,B.A. and Manke,T. (2014) deepTools: a flexible platform for exploring deep-sequencing data. *Nucleic Acids Res.*, **42**, W187–W191.

41. Egli,D., Domenech,J., Selvaraj,A., Balamurugan,K., Hua,H., Capdevila,M., Georgiev,O., Schaffner,W. and Atrian,S. (2006) The four members of the drosophila metallothionein family exhibit distinct yet overlapping roles in heavy metal homeostasis and detoxification. *Genes Cells*, **11**, 647–658.

42. Smale,S.T. (2009) Nuclear run-on assay. *Cold Spring Harb. Protoc.*, **2009**, pdb prot5329.

43. Roberts,T.C., Hart,J.R., Kaikkonen,M.U., Weinberg,M.S., Vogt,P.K. and Morris,K.V. (2015) Quantification of nascent transcription by bromouridine immunocapture nuclear run-on RT-qPCR. *Nat. Protoc.*, **10**, 1198–1211.

44. Chen,L., Huang,C. and Shan,G. (2022) Circular RNAs in physiology and non-immunological diseases. *Trends Biochem. Sci*, **47**, 250–264.

45. Chen,X., Zhou,M., Yant,L. and Huang,C. (2022) Circular RNA in disease: basic properties and biomedical relevance. *Wiley Interdiscip. Rev. RNA*, e1723.

46. Zhou,M., Xiao,M.S., Li,Z. and Huang,C. (2021) New progresses of circular RNA biology: from nuclear export to degradation. *RNA Biol.*, **18**, 1365–1373.

47. Huang,C., Liang,D., Tatomer,D.C. and Wilusz,J.E. (2018) A length-dependent evolutionarily conserved pathway controls nuclear export of circular RNAs. *Genes Dev.*, **32**, 639–644.

48. Cramer,P. (2019) Organization and regulation of gene transcription. *Nature*, **573**, 45–54.

49. Hwang,S., Gou,Z. and Kuznetsov,I.B. (2007) DP-Bind: a web server for sequence-based prediction of DNA-binding residues in DNA-binding proteins. *Bioinformatics*, **23**, 634–636.

50. Talbert,P.B., Meers,M.P. and Henikoff,S. (2019) Old cogs, new tricks: the evolution of gene expression in a chromatin context. *Nat. Rev. Genet.*, **20**, 283–297.

51. Gao,R., Helfant,L.J., Wu,T., Li,Z., Brokaw,S.E. and Stock,A.M. (2021) A balancing act in transcription regulation by response regulators: titration of transcription factor activity by decoy DNA binding sites. *Nucleic Acids Res.*, **49**, 11537–11549.

52. Li,G. and Reinberg,D. (2011) Chromatin higher-order structures and gene regulation. *Curr. Opin. Genet. Dev.*, **21**, 175–186.

53. Luger,K., Dechassa,M.L. and Tremethick,D.J. (2012) New insights into nucleosome and chromatin structure: an ordered state or a disordered affair? *Nat. Rev. Mol. Cell Biol.*, **13**, 436–447.

54. Cao,J., Luo,Z., Cheng,Q., Xu,Q., Zhang,Y., Wang,F., Wu,Y. and Song,X. (2015) Three-dimensional regulation of transcription. *Protein Cell*, **6**, 241–253.

55. Warner,D.R., Bhattacherjee,V., Yin,X., Singh,S., Mukhopadhyay,P., Pisano,M.M. and Greene,R.M. (2004) Functional interaction between smad, CREB binding protein, and p68 RNA helicase. *Biochem. Biophys. Res. Commun.*, **324**, 70–76.

56. Rossow,K.L. and Janknecht,R. (2003) Synergism between p68 RNA helicase and the transcriptional coactivators CBP and p300. *Oncogene*, **22**, 151–156.

57. Wilson,B.J., Bates,G.J., Nicol,S.M., Gregory,D.J., Perkins,N.D. and Fuller-Pace,F.V. (2004) The p68 and p72 DEAD box RNA helicases interact with HDAC1 and repress transcription in a promoter-specific manner. *BMC Mol. Biol.*, **5**, 11.

58. Lambert,M.P., Terrone,S., Giraud,G., Benoit-Pilven,C., Cluet,D., Combaret,V., Mortreux,F., Auboeuf,D. and Bourgeois,C.F. (2018) The RNA helicase DDX17 controls the transcriptional activity of REST and the expression of proneural microRNAs in neuronal differentiation. *Nucleic Acids Res.*, **46**, 7686–7700.

59. Zhang,H., Xing,Z., Mani,S.K., Bancel,B., Durantel,D., Zoulim,F., Tran,E.J., Merle,P. and Andrisani,O. (2016) RNA helicase DEAD box protein 5 regulates polycomb repressive complex 2/Hox transcript antisense intergenic RNA function in hepatitis b virus infection and hepatocarcinogenesis. *Hepatology*, **64**, 1033–1048.

60. Chereji,R.V., Bryson,T.D. and Henikoff,S. (2019) Quantitative MNase-seq accurately maps nucleosome occupancy levels. *Genome Biol.*, **20**, 198.

61. Yu,J., Xiong,C., Zhuo,B., Wen,Z., Shen,J., Liu,C., Chang,L., Wang,K., Wang,M., Wu,C. *et al.* (2020) Analysis of local chromatin states reveals gene transcription potential during mouse neural progenitor cell differentiation. *Cell Rep.*, **32**, 107953.

62. Legrand,J.M.D., Chan,A.L., La,H.M., Rossello,F.J., Anko,M.L., Fuller-Pace,F.V. and Hobbs,R.M. (2019) DDX5 plays essential transcriptional and post-transcriptional roles in the maintenance and function of spermatogonia. *Nat. Commun.*, **10**, 2278.

63. Cheng,H., Dufu,K., Lee,C.S., Hsu,J.L., Dias,A. and Reed,R. (2006) Human mRNA export machinery recruited to the 5′ end of mRNA. *Cell*, **127**, 1389–1400.

64. Gatfield,D., Le Hir,H., Schmitt,C., Braun,I.C., Kocher,T., Wilm,M. and Izaurralde,E. (2001) The DExH/D box protein HEL/UAP56 is essential for mRNA nuclear export in drosophila. *Curr. Biol.*, **11**, 1716–1721.

65. Taniguchi,I. and Ohno,M. (2008) ATP-dependent recruitment of export factor Aly/REF onto intronless mRNAs by RNA helicase UAP56. *Mol. Cell. Biol.*, **28**, 601–608.

66. Wang,Y., Arribas-Layton,M., Chen,Y., Lykke-Andersen,J. and Sen,G.L. (2015) DDX6 orchestrates mammalian progenitor function through the mRNA degradation and translation pathways. *Mol. Cell*, **60**, 118–130.

67. Fasken,M.B. and Corbett,A.H. (2009) Mechanisms of nuclear mRNA quality control. *RNA Biol.*, **6**, 237–241.

68. Schmid,M. and Jensen,T.H. (2018) Controlling nuclear RNA levels. *Nat. Rev. Genet.*, **19**, 518–529.

69. Porrua,O. and Libri,D. (2013) RNA quality control in the nucleus: the angels' share of RNA. *Biochim. Biophys. Acta*, **1829**, 604–611.

70. Zander,G., Hackmann,A., Bender,L., Becker,D., Lingner,T., Salinas,G. and Krebber,H. (2016) mRNA quality control is bypassed for immediate export of stress-responsive transcripts. *Nature*, **540**, 593–596.

71. Perez-Calero,C., Bayona-Feliu,A., Xue,X., Barroso,S.I., Munoz,S., Gonzalez-Basallote,V.M., Sung,P. and Aguilera,A. (2020) UAP56/DDX39B is a major cotranscriptional RNA-DNA helicase that unwinds harmful r loops genome-wide. *Genes Dev.*, **34**, 898–912.